A Two-Octave GaN Power Amplifier based on a Multi-Section Chebyshev Transformer

Reza Koliaei
Politecnico di Torino
Turin, Italy
Reza.Koliaei@studenti.polito.it

Giulia Bartolotti
Politecnico di Torino
Turin, Italy
Giulia.Bartolotti@polito.it

Zhifan Zhang
Politecnico di Torino
Turin, Italy
Zhifan.Zhang@polito.it

Anna Piacibello
Politecnico di Torino
Turin, Italy
Anna.Piacibello@polito.it

Vittorio Camarchia
Politecnico di Torino
Turin, Italy
Vittorio.Camarchia@polito.it

***Abstract*—This paper presents the design and characterization of an ultra-wideband (0.8 GHz–3.2 GHz) hybrid single-stage class-AB power amplifier based on a 25-W packaged GaN device. Over this two-octave bandwidth, the amplifier reaches saturated output power higher than 42 dBm with associated efficiency above 53%. An output matching network consisting of a 4-section Chebyshev transformer has been implemented based on the optimum load trajectory, targeting a trade-off between output power and efficiency.**

***Index Terms*—Broadband matching networks, GaN-based FETs, wideband microwave amplifiers.**

I. Introduction

Modern communication systems are heavily dependent on broadband power amplifiers (PA), which allow high-performance signal transmission over various frequency bands. Rapid development of wireless communication technologies, such as 5G networks, satellite communication, radar systems, and software-defined radios, has led to a huge increase in the demand for broadband operation. High power delivery, linearity, and efficient operation across wide frequency bands are requirements for these applications.

Several broadband PA designs are available in the literature (see Table I). In [1], a lumped element multistage low pass Chebyshev network has been utilized to reach a fractional bandwidth of 90% and output power of 25 W. In [2], a class-GF PA is introduced that achieves 10 W output power on a multi-octave bandwidth, from 0.4 GHz up to 2.8 GHz, by fundamental and second harmonic manipulation. The design in [3], adopts a prediction of power and efficiency contours based on the knee profile of the device and then realizes optimum load trajectory by adjusting real to real matching network followed by drain stub to compensate for low-frequency response. In [4], the design strategy utilizes negative feedback to achieve a wide bandwidth while maintaining minimum gain and efficiency imbalance.

This work adopts a 25-W CGH40025F GaN HEMT device and aims at achieving efficient power amplification over a two-octave bandwidth (0.8–3.2 GHz). The use of a packaged GaN device [5], [6] enables achieving the required power level while maintaining wideband performance within a single device. Based on the trade-off between efficiency and power contours at different frequencies and considering the partial overlap between fundamental and second harmonic frequency ranges, an optimum load trajectory is selected and synthesized by means of a 4-section real-to-real matching network following the compensation of the device parasitic effects performed by the drain stub.

TABLE I: Recent ultra-wideband PAs summary.

Ref.	Freq. (GHz)	BW (%)	Out. power (dBm)	Gain (dB)	Efficiency (%)
[1]	0.9–2.4	90	40–44	17–23	25–78
[2]	0.4–2.8	150	39–42	9–12	63–73
[3]	0.45–3.4	153.2	42–44.3	8–10.5	54–70.4*
[4]	0.33–3.7	167	42–44.8	7.2–12.2	58–71
T. W.	**0.8–3.2**	**120**	**42–44.7**	**9.8–17.9**	**53–67**

* refers to PAE

II. Design Procedure

A. Active Device Selection

The 25-W CGH40025F GaN HEMT from Wolfspeed is selected and biased in class AB at gate voltage of -2.8 V and drain voltage of 28 V. As a result, the drain current is around 0.31 A. In these conditions, the intrinsic optimum load is around 12 Ω [3]. As the active device periphery increases, to achieve higher power, the design of the PA becomes more challenging because the optimum load reduces in magnitude making the design of wideband output matching network harder. The target efficiency and output power for this work are higher than 50% and 43 dBm, respectively.

B. Optimum Terminations

The biggest challenge in designing a broadband PA is the optimum load variation due to the dispersive behavior of the transistor's parasitics with respect to frequency. While

harmonic control is often an effective strategy to enhance the PA's output power and efficiency, in broadband designs higher-order harmonics of the lower frequencies may fall inside the desired bandwidth. In this design, in the higher frequency band (1.6 GHz–3.2 GHz) harmonics are terminated with high impedance values in load-pull simulations like in [7]. Starting from 3.2 GHz with a frequency spacing of 200 MHz, we obtain optimum fundamental load impedances based on the best trade-off between output power and efficiency. From 1.6 GHz as we decrease the frequency, higher order harmonics fall inside the higher frequency band (1.6 GHz–3.2 GHz), hence by replacing optimum impedance values obtained in the previous step as higher order harmonic terminations in load-pull simulations and considering the best trade-off between output power and efficiency, we obtain the desired impedance values for the lower frequency band as well.

Fig. 1 shows the effect of the sub-optimal second harmonic termination at 0.8 GHz, where it causes earlier saturation, and 1.6 GHz, where it negatively affects the maximum achievable efficiency.

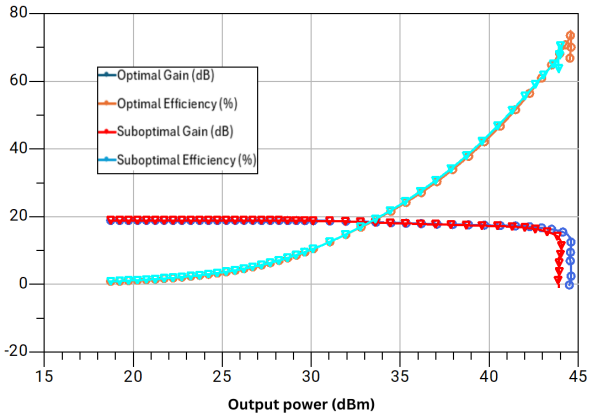

(a)

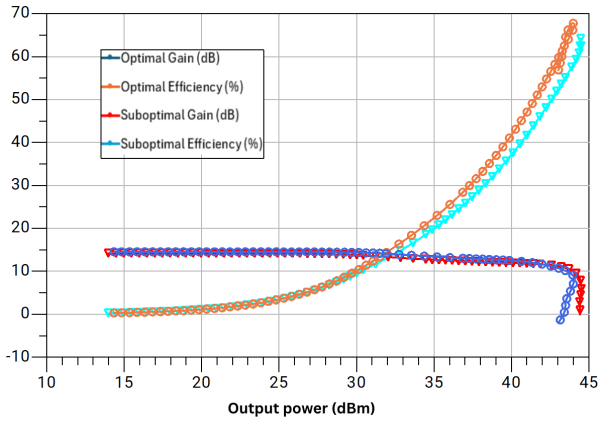

(b)

Fig. 1: Simulated gain and efficiency versus output power under optimal and suboptimal second harmonic termination at (a) 0.8 GHz and (b) 1.6 GHz.

Fig. 2 shows the target and synthesized load trajectories, superimposed on constant efficiency and power contours at different frequencies. The synthesized second harmonic terminations (3.2 GHz–6.4 GHz) are slightly further away from target ones due to the selection of a 4-section matching network for minimizing PCB area. However, the synthesized second harmonic loads do not significantly deteriorate the overall performance.

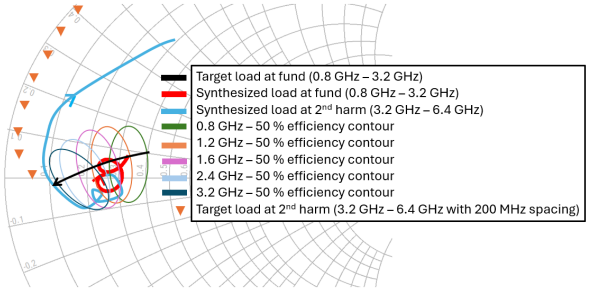

(a)

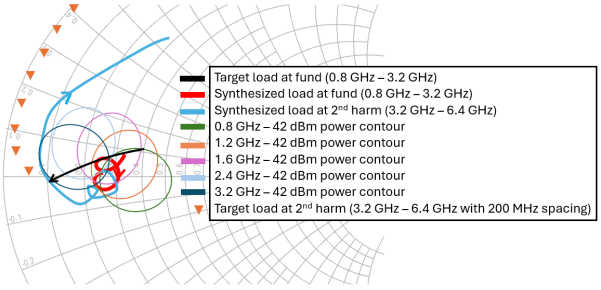

(b)

Fig. 2: Comparison between target and synthesized loads at fundamental and second harmonic, superimposed on (a) 50%-efficiency and (b) 42-dBm power contours.

Based on the selection of the optimum load trajectory, without considering losses due to either dissipation or mismatch, it is expected that power-added efficiency (PAE) and output power will reach higher than 55% and 44 dBm, respectively.

C. OMN Design Strategy

The design strategy for the OMN is to use the drain bias line not only for the DC drain path but also to compensate for the output parasitics of the transistor, and then adopt a multi-section real-to-real impedance transformer to match the optimum output resistance to 50 Ω. The proposed topology consists of N cascaded 90° transmission lines based on the Chebyshev matching response centered at $f_0 = 2$ GHz with in-band reflection of -10 dB. Based on the theory of small reflections and Chebyshev polynomials, the desired reflection is (1) [8]:

$$\Gamma(\theta) = A \cdot e^{-jN\theta} \cdot T_N(\sec\theta_m \cdot cos\theta), \qquad (1)$$

where A is the in-band reflection magnitude, N is the number of sections, θ is the phase of the reflection coefficient and θ_m

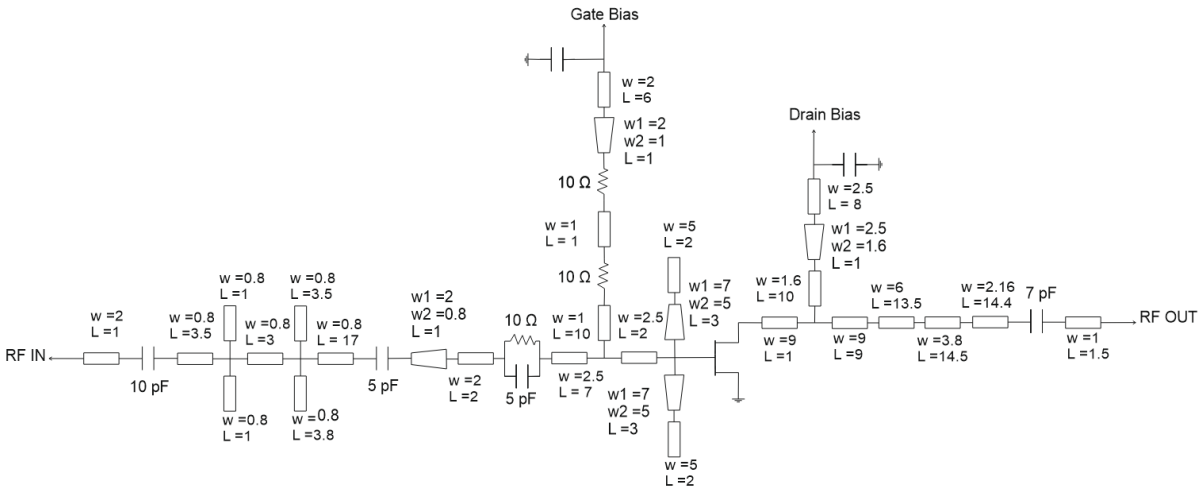

Fig. 3: Schematic of the proposed PA (dimensions are in mm).

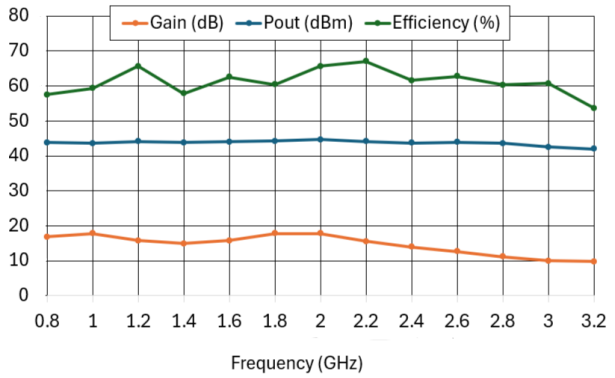

Fig. 4: Measured small signal gain, saturated output power and saturated efficiency versus frequency.

is the reflection coefficient phase at the lower band edge. It results that 4 sections network can provide a bandwidth of $\left[\frac{1}{3}\frac{f}{f_0}, \frac{5}{3}\frac{f}{f_0}\right]$ with $A = 0.1$, which is sufficient for our target band.

The theoretical ratios of the characteristic impedance of each section relative to the optimum resistance ($Z_0 = 12\,\Omega$) result:

$$\frac{Z_1}{Z_0} = 1.19 \quad \frac{Z_2}{Z_0} = 1.64 \quad \frac{Z_3}{Z_0} = 2.44 \quad \frac{Z_4}{Z_0} = 3.36. \qquad (2)$$

III. Realization and Characterization

Fig. 3 presents the complete PA schematic. This circuit is constructed on a Rogers 4350B substrate with dielectric constant of 3.66, and thickness of 0.76 mm. The input matching network is composed of a DC blocking capacitor, four high-impedance open stubs, another series capacitor, and two low-impedance open stubs to achieve a reasonable trade-off between minimum reflection and gain variations over the entire bandwidth. In-band stabilization is achieved through a series RC network, while for low-frequency stability, two resistors in the gate bias line have been chosen. Fig. 5 shows the manufactured ultra wideband PA.

The experimental results in terms of small signal gain, saturated output power and efficiency versus frequency are shown in Fig. 4. The output power varies between 42 dBm and 44.7 dBm and the resulting efficiency is between 53% and 67% in a 120% fractional bandwidth (0.8 GHz–3.2 GHz). Compared to the state of the art summarized in Table I, this PA achieves power and efficiency comparable to [1], [3], [4], which adopts the same active device, with a slightly higher gain. Compared to [2], which adopts a smaller device, the bandwidth is slightly narrower as the optimum load of the 25 W device deviates more significantly from 50 Ω, but the gain and efficiency performance is still competitive while delivering an output power that is almost doubled.

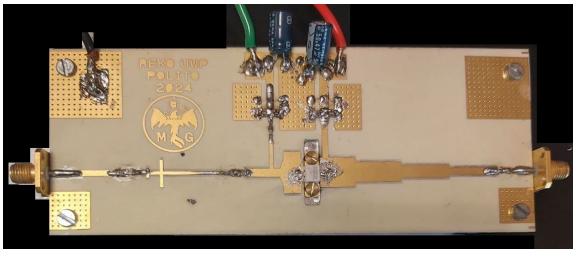

Fig. 5: Photograph of the proposed PA (4.5 cm × 12.4 cm).

IV. Conclusion

In this work, an ultra-wideband PA operating over mid-band has been introduced. The design methodology adopts a 4 section Chebyshev matching network to ensure the operating frequency range between 0.8 GHz up to 3.2 GHz with the efficiency between 53% and 67% and output power of higher than 42 dBm up to 44.7 dBm.

REFERENCES

[1] T. B. Rashid and H. Song, "A wideband 0.9–2.4 GHz 25 W high-efficiency Gallium Nitride radio frequency power amplifier," *Engineering Reports*, vol. 3, no. 8, p. e12386, 2021.

[2] X. Xuan, Z. Cheng, Z. Zhang, T. Gong, G. Liu, and C. Le, "Design of an extended continuous-mode class-GF power amplifier with multioctave bandwidth," *IEEE Microwave and Wireless Technology Letters*, 2023.

[3] J. J. M. Rubio, R. Quaglia, A. Baddeley, P. J. Tasker, and S. C. Cripps, "Design of a broadband power amplifier based on power and efficiency contour estimation," *IEEE Microwave and Wireless Components Letters*, vol. 30, no. 8, pp. 772–774, 2020.

[4] D. Li, F. Yang, C. Guo, and X. Li, "An Ultrawideband Power Amplifier Based on Negative Feedback," *IEEE Microwave and Wireless Technology Letters*, 2024.

[5] V. Camarchia, S. D. Guerrieri, M. Pirola, V. Teppati, A. Ferrero, G. Ghione, M. Peroni, P. Romanini, C. Lanzieri, S. Lavanga, A. Serino, E. Limiti, and L. Mariucci, "Fabrication and nonlinear characterization of GaN HEMTs on SiC and sapphire for high-power applications," *International Journal of RF and Microwave Computer-Aided Engineering*, vol. 16, no. 1, pp. 70–80, 2006.

[6] R. S. Pengelly, S. M. Wood, J. W. Milligan, S. T. Sheppard, and W. L. Pribble, "A Review of GaN on SiC High Electron-Mobility Power Transistors and MMICs," *IEEE Transactions on Microwave Theory and Techniques*, vol. 60, no. 6, pp. 1764–1783, 2012.

[7] M. Iqbal and A. Piacibello, "A 5W class-AB power amplifier based on a GaN HEMT for LTE communication band," in *2016 16th Mediterranean Microwave Symposium (MMS)*, 2016, pp. 1–4.

[8] D. M. Pozar, *Microwave engineering: theory and techniques*. John wiley & sons, 2021.

[9] M. Ghazizadeh and V. Nayyeri, "Design of a 50-W power amplifier with two-octave bandwidth and high-efficiency using a systematic optimization approach," *IEEE Microwave and Wireless Components Letters*, vol. 31, no. 5, pp. 501–504, 2021.

[10] J. J. M. Rubio, V. Camarchia, R. Quaglia, E. F. A. Malaver, and M. Pirola, "A 0.6–3.8 GHz GaN power amplifier designed through a simple strategy," *IEEE Microwave and Wireless Components Letters*, vol. 26, no. 6, pp. 446–448, 2016.

[11] A. Nasri, M. Estebsari, S. Toofan, A. Piacibello, C. Ramella, V. Camarchia, and M. Pirola, "A 3-3.8 GHz Class-J GaN HEMT Power Amplifier," in *2020 23rd International Microwave and Radar Conference (MIKON)*, 2020, pp. 416–419.

[12] A. Piacibello, J. J. Moreno Rubio, R. Quaglia, and V. Camarchia, "AM/PM Characterization of Wideband Power Amplifiers," in *2022 IEEE Topical Conference on RF/Microwave Power Amplifiers for Radio and Wireless Applications (PAWR)*, 2022, pp. 82–85.

[13] J. J. M. Rubio, R. Quaglia, A. Piacibello, V. Camarchia, P. J. Tasker, and S. Cripps, "3–20-GHz GaN MMIC Power Amplifier Design Through a COUT Compensation Strategy," *IEEE Microwave and Wireless Components Letters*, vol. 31, no. 5, pp. 469–472, 2021.